# MULTISCALE RICIAN APPROACH TO GABOR FILTER DESIGN FOR TEXTURE SEGMENTATION

*Thomas P. Weldon and William E. Higgins*

Department of Electrical Engineering
The Pennsylvania State University, University Park, PA 16802
E-mail: weh@ruth.ece.psu.edu

## ABSTRACT

Gabor filters have been applied successfully to the segmentation of textured images. Previous investigators have used banks of Gabor filters, where the filter parameters were predetermined *ad hoc* and not necessarily optimized for a particular task. Other investigators have proposed using filters tuned to dominant components in the FFT of constituent textures. More recent work presented a Gabor filter design method using a Rician distribution to characterize the filtered textures. The present work addresses the design of a single Gabor filter to segment multiple textures and is based on using the Rician distribution at two different scales of the Gabor-filter envelope. Furthermore, variable degrees of postfiltering and the accompanying effect on postfilter output statistics are considered.

## 1. INTRODUCTION

[1] Texture segmentation is the process of partitioning an image into regions of different texture. Gabor filters have been employed successfully in filter-based texture-segmentation schemes because (1) they provide optimal joint resolution in the space and spatial-frequency domains, and (2) they are bandpass filters, conforming well to the human visual system [1, 2]. Previous investigators employed banks of Gabor filters for texture segmentation [3, 4]. The configurations of Gabor filters making up the filter-banks were predetermined *ad hoc*, however, and were not optimized for a given application. Other researchers have proposed filter bank schemes based on a large number of bandpass filters similar to the Gabor filter: difference of offset Gaussians [5], prolate spheroid functions [6], wavelet transform [7], and subband decomposition [8]. These schemes also used predetermined fixed filters or filters with available bandwidths dependent on center frequency.

Recent work has focused on designing one or a few Gabor filters for a particular application in an effort to reduce the computional burden and to improve the segmentation performance [2, 9–11]. Bovik *et al.* proposed designing Gabor filters that focused on the dominant spatial-frequency components in the FFT of constituent textures. More recently, optimal methods for designing a single Gabor filter have been developed for the two-texture segmentation problem [10, 11]. These methods search for the Gabor filter minimizing the image-segmentation error by modelling the output statistics of a Gabor-filtered texture with a Rician distribution. Two major issues still remain: (1) how to design a single Gabor filter optimally for the multi-texture case; and (2) how to design multiple Gabor filters optimally.

This paper presents a method for designing a Gabor filter for the multi-texture case (issue 1) and can lead to the design of multiple Gabor filters (issue 2). The single-filter multi-texture design problem with variable postfiltering has not been addressed by previous investigators. The present method employs a Rician Gabor-filter output model at multiple scales to generate estimates of candidate filter output statistics and associated texture-segmentation error. The predicted segmentation error is then used to design the optimal Gabor filter. Multiple filters may be necessary to handle complex multi-texture segmentation problems. The proposed approach to the single-filter design problem leads to the design of multiple Gabor filters, because the output statistics for all textures are estimated for an exhaustive set of candidate filters.

## 2. PROBLEM OVERVIEW

The image processing under consideration is shown in Fig. 1 and is similar to the scheme for two textures

used in [11]. The technique outlined in the figure has been justified for texture segmentation by previous investigators [9,12]. We now review the image-processing scheme and define the texture-segmentation problem.

The input image $i(x,y)$ is assumed to be composed of two or more textures. First, the input $i(x,y)$ is filtered using a bandpass Gabor prefilter with impulse response $h(x,y)$:

$$h(x,y) \quad = \quad g(x,y)\, e^{-j2\pi(Ux+Vy)} \tag{1}$$

where

$$g(x,y) \quad = \quad \frac{1}{2\pi\sigma_g^2}\, e^{-\frac{(x^2+y^2)}{2\sigma_g^2}}\ , \tag{2}$$

and $g(x,y)$ is assumed to be circularly symmetric for simplicity. The Gabor prefilter function $h(x,y)$, referred to as a Gabor function, is a complex sinusoid at frequency $(U,V)$ modulated by a Gaussian envelope $g(x,y)$ [2]. The spatial-frequency response $H(u,v)$ of the Gabor prefilter is:

$$H(u,v) \quad = \quad G(u-U, v-V) \tag{3}$$

where

$$G(u,v) \quad = \quad e^{-2\pi^2\sigma_g^2(u^2+v^2)}\ . \tag{4}$$

The Gabor function is essentially a bandpass filter centered about frequency $(U,V)$, with bandwidth determined by $\sigma_g$. We will refer to $(U,V)$ as the *center frequency* of the Gabor prefilter. The spatial extent, or *scale*, of $h(x,y)$ is also determined by $\sigma_g$. More precisely, $\sigma_g$ determines the scale of the envelope of $h(x,y)$; it does not scale the center frequency. Continuing the description of Fig. 1, the Gabor prefilter output is:

$$i_h(x,y) = h(x,y) ** i(x,y) \tag{5}$$

where $**$ denotes two-dimensional convolution.

The magnitude of the prefiltered image is:

$$m(x,y) = |i_h(x,y)| = |\ h(x,y) ** i(x,y)\ | \tag{6}$$

where $m(x,y)$ has been shown to have approximately Rician statistics within the extent of each texture [10, 11]. A low-pass Gaussian postfilter $g_p(x,y)$ is then applied, yielding the postfiltered image:

$$m_p(x,y) \quad = \quad m(x,y) ** g_p(x,y) \tag{7}$$

where

$$g_p(x,y) \quad = \quad \frac{1}{2\pi\sigma_p^2}\, e^{-\frac{(x^2+y^2)}{2\sigma_p^2}}\ . \tag{8}$$

It has been well established that the Gaussian postfilter reduces the error in texture segmentation [9]. In particular, $m_p(x,y)$ has a smaller variance than $m(x,y)$, and, therefore, lowers the texture-discrimination error [11].

As a final processing step, the segmented image $i_s(x,y)$ is generated by applying several thresholds to the postfiltered image $m_p(x,y)$. More elaborate methods can be used to generate the segmented image from the postfiltered image, but a simple threshold scheme more directly illustrates the efficacy of our methods.

Given the system of Fig. 1, the goal is to design the Gabor prefilter $h(x,y)$ and Gaussian postfilter $g_p(x,y)$ such that the resulting aggregate segmentation error for all texture classes in $m_p(x,y)$ is minimized. Our approach can be summarized as follows.
(1) Given samples of the textures of interest $t_i(x,y)$, $i = 1,\ldots,N$, estimate the associated Rician statistics of $m(x,y)$ for each texture, over a range of Gabor filter center frequencies $(U,V)$ and scales $\sigma_g$.
(2) Estimate the approximately Gaussian-distributed statistics of the postfilter output $m_p(x,y)$ using the results generated in step 1; this gives a Gaussian distributed $m_p(x,y)$ for each $t_i$.
(3) Compute a series of optimal thresholds that can be applied to $m_p(x,y)$ and compute the associated segmentation error assuming equal *a priori* probabilities.
(4) Select the Gabor prefilter, determined by $(U,V,\sigma_g)$, and Gaussian postfilter, determined by $\sigma_p$, that give the lowest aggregate segmentation rate at an acceptable resolution.

Additional detail follows.

## 3. FILTER DESIGN METHOD

Previous results have shown that the output statistics of $m(x,y)$ often are well modeled by a Rician pdf. This suggests that the prefilter output $i_h(x,y)$ for texture $t_i$ may be modeled as a dominant complex sinusoid with amplitude $A_i$ at spatial frequency $(u_i, v_i)$ plus noise [11,13] :

$$i_{hi}(x,y) \quad \approx \quad A_i\, e^{j2\pi(u_i\, x+v_i\, y)} + n_i(x,y) \tag{9}$$

where the subscript $i$ indicates that this is the prefilter output model for texture $t_i(x,y)$. Now, consider $i_{hi}(x,y)$ to be the prefiltered version of the following input power spectrum of an ergodic process:

$$S_i(u,v) \approx A_i^2\delta(u-u_i, v-v_i) + \frac{\eta_i}{4} \tag{10}$$

where the impulse $\delta(\cdot)$ in the power spectrum models the dominant sinusoid within the filter passband, and the remaining power in the passband is allocated to $\eta_i/4$. We emphasize that this model is only valid within the approximate passband of the prefilter, i.e., it is a *locally* equivalent model in the spatial-frequency plane for an input texture $t_i(x,y)$.

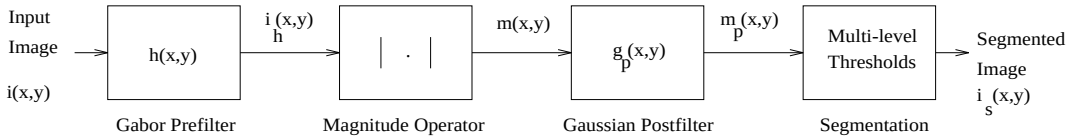


Figure 1: Image processing block diagram.

Now, consider (10) convolved with:

$$|G(u,v)|^2 = \mathcal{F}\{g(x,y) * * g(x,y)\} \tag{11}$$

where $\mathcal{F}\{\cdot\}$ denotes the Fourier transform operator, and $g(x,y)$ is from (2). We obtain the following measure of prefilter output power as a function of prefilter center frequency:

$$\begin{aligned} P_i(u,v,\sigma_g) &\approx |G(u,v)|^2 * * S_i(u,v) \\ &\approx A^2{}_i \; e^{-4\pi^2\sigma_g^2[(u-u_i)^2+(v-v_i)^2]} + \frac{\eta_i}{16\pi\sigma_g^2} \end{aligned} \tag{12}$$

The first term above arises from the dominant sinusoid in the passband represented by the impulse in (10). From Parseval's theorem, $P_i(u,v,\sigma_g)$ may be interpreted as the total power of $i_{hi}(x,y)$ for a Gabor prefilter with center frequency $(u,v)$ and parameter $\sigma_g$. Relation (12) can be efficiently implemented in a discretized form using the FFT. The discrete form then gives $P_i(u,v,\sigma_g)$ at a discrete set of center frequencies $(u,v)$ and a particular $\sigma_g$. The second term represents the remaining output power of the Gabor prefilter and gives the parameter $N_i = \eta_i/(16\pi\sigma_g^2)$ in the Rician pdf $p_i(m)$ of $m(x,y)$ for texture $t_i$ [10, 11]:

$$p_i(m) = \frac{2m}{N_i}\, e^{-(\frac{m^2+A_i^2}{N_i})}\, I_0(\frac{2mA_i}{N_i}) \tag{13}$$

where $m = m(x,y)$ for input texture $t_i(x,y)$, $A_i$ is the amplitude of the dominant sinusoid, $N_i$ is the total noise power, and $I_0(\cdot)$ is the modified Bessel function of the first kind with zero order. The Rician distribution is completely determined by the values of $A_i$ and $N_i$.

If we next consider $P_i(u,v,\sigma_g)$ at two prefilter envelope scales set by $\sigma_{g\alpha}$ and $\sigma_{g\beta}$, we may solve for $N_i$ and $A_i$ at the frequency $(u_i,v_i)$ of the dominant sinusoid:

$$\begin{aligned} P_i(u,v,\sigma_{g\alpha}) &\approx A_i^2 + \frac{\eta_i}{16\pi\sigma_{g\alpha}^2} \\ P_i(u,v,\sigma_{g\beta}) &\approx A_i^2 + \frac{\eta_i}{16\pi\sigma_{g\beta}^2} \end{aligned} \tag{14}$$

rearranging:

$$N_i(u,v,\sigma_{g\alpha}) \approx \frac{P_i(u,v,\sigma_{g\alpha}) - P_i(u,v,\sigma_{g\beta})}{[1-(\frac{\sigma_{g\alpha}}{\sigma_{g\beta}})^2]} \tag{15}$$

and

$$A_i^2(u,v,\sigma_{g\alpha}) \approx P_i(u,v,\sigma_{g\alpha}) - N_i(u,v,\sigma_{g\alpha}). \tag{16}$$

As the prefilter center frequency diverges from $(u_i,v_i)$, the exponential term in (12) becomes less than 1, and error can be introduced in (14), (15), and (16), particularly for $\eta_i = 0$. (Note that for $A_i = 0$ this error does not arise.) Examination of (12), (15), and (16) for $\eta_i = 0$ shows that as the exponential term in (12) becomes less than 1, power is increasingly attributed to $N_i$ when in fact $N_i$ should equal 0. The net effect of this error, however, is beneficial in the overall algorithm. The error induces a preference for the frequency $(u_i,v_i)$ of the local dominant sinusoid, since lower $N_i$ implies lower variance in $m_p(x,y)$. Hence, the following equations are used to estimate $N_i$ and $A_i$ for all $(u,v)$:

$$N_i(u,v,\sigma_{g\alpha}) \approx \frac{P_i(u,v,\sigma_{g\alpha}) - P_i(u,v,\sigma_{g\beta})}{[1-(\frac{\sigma_{g\alpha}}{\sigma_{g\beta}})^2]} \tag{17}$$

and

$$A_i^2(u,v,\sigma_{g\alpha}) \approx P_i(u,v,\sigma_{g\alpha}) - N_i(u,v,\sigma_{g\alpha}) \tag{18}$$

Since $A_i$ and $N_i$ determine the Rician pdf, means $\mu_{gi}$ and variances $s_{gi}^2$ of $m(x,y)$ may be calculated directly for each sample texture $t_i(x,y)$. The postfilter means $\mu_{pi}$ and variances $s_{pi}^2$ for texture $t_i$ are derived from the prefilter means and variances using the parameters $\sigma_g$ and $\sigma_p$ (with an increasingly Gaussian distribution for large $\frac{\sigma_p}{\sigma_g}$) :

$$\begin{aligned} \mu_{p_i}(u,v) &= \mu_{gi}(u,v) \\ s_{p_i}^2(u,v) &= \frac{s_{gi}^2(u,v)\;\sigma_g^2}{\sigma_p^2} \end{aligned} \tag{19}$$

The foregoing procedure for estimating the postfilter output means and variances is repeated for representative samples of all textures of interest. A series of optimal segmentation thresholds are calculated based on the assumption of a multi-modal Gaussian pdf and equal *a priori* probabilities for the textures. Thresholds are selected that minimize the total segmentation error. Stated another way, thresholds are set such that $m_p(x,y)$ is assigned to the texture whose probability

density is largest for a given output level. Assuming equal *a priori* probabilities for the $N$ textures, the minimum segmentation error rate is achieved by deciding texture $t_i$ when [14]:

$$p_i(u,v,m_p) > p_j(u,v,m_p)\,; \quad j \neq i,\ 1 \leq i,j \leq N \quad (20)$$

where the estimated Gaussian pdf $p_i(u,v,m_p)$ of the postfiltered output $m_p(x,y)$ for texture $t_i(x,y)$ is:

$$p_i(u,v,m_p) = \frac{1}{\sqrt{2\pi s^2_{p_i}(u,v)}}\, e^{-\frac{(m_p - \mu_{p_i}(u,v))^2}{2s^2_{p_i}(u,v)}} \quad (21)$$

Using these thresholds, the segmentation error is estimated for each candidate Gabor filter. The filter giving the lowest segmentation error is selected.

## 4. RESULTS

Sample results are shown in Fig. 2 for a 256x256 image composed of two Brodatz textures and a random texture [15]. The input image shown in Fig. 2a consists of a central region of texture d77 embedded in a larger region composed of texture d15 imposed on a background of uniformly distributed random noise. Three 256x256 samples of the textures were used to design the Gabor prefilter. For illustration, single values of $\sigma_g$ and $\sigma_p$ are considered. The magnitude of the optimal Gabor prefilter output $m(x,y)$ is shown in Fig. 2b. The predicted and actual histograms for $m(x,y)$ are in Fig. 2c. Fig. 2d is the thresholded version of the postfiltered output $m_p(x,y)$. The predicted and actual statistics for $m_p(x,y)$ are in Fig. 2e. Note that even though the predicted and measured distributions may differ, the thresholds are effective. Finally, Fig. 2f is a plot of the predicted segmentation error as a function of Gabor prefilter center frequency $(U,V)$ with a white intensity indicating a segmentation error of 100%, and black 0%. The prominent dark ring in Fig. 2f is due to a lowpass filter operation on each of the original Brodatz images to eliminate high frequency artifacts [16]. The darkest point in the image corresponds to the prefilter center frequency for this example. Clearly, as we see from Fig. 2d, the method produced a Gabor prefilter that gives good segmentation of a difficult image.

## 5. REFERENCES


[1] J. G. Daugman, "Uncertainty relation for resolution in space, spatial frequency, and orientation optimized by two-dimensional visual cortical filters," *J. Opt. Soc. Amer. A*, vol. 2, no. 7, pp. 1160–69, July 1985.

[2] A. C. Bovik, M. Clark, and W. S. Geisler, "Multichannel texture analysis using localized spatial filters," *IEEE Trans. Pattern Anal. Machine Intell.*, vol. 12, no. 1, pp. 55–73, Jan. 1990.

[3] J. G. Daugman, "Complete discrete 2-D Gabor transforms by neural networks for image analysis and compression," *IEEE Trans. Acoust., Speech, Signal Processing*, vol. 36, no. 7, pp. 1169–79, July 1988.

[4] A. K. Jain and F. Farrokhnia, "Unsupervised texture segmentation using Gabor filters," *Pattern Recognition*, vol. 23, no. 12, pp. 1167–86, Dec. 1991.

[5] J. Malik and P. Perona, "Preattentive texture discrimination with early vision mechanisms," *J. Opt. Soc. Amer. A*, vol. 7, no. 5, pp. 923–32, May 1990.

[6] R. Wilson and M. Spann, "Finite prolate spheroidal sequences and their applications II: Image feature description and segmentation," *IEEE Trans. Pattern Anal. and Machine Intell.*, vol. 10, no. 2, pp. 193–203, Mar. 1988.

[7] T. Chang and C. C. J. Kuo, "Texture analysis and classification with tree-structured wavelet transform," *IEEE Trans. Image Proc.*, vol. 2, no. 4, pp. 429–441, Oct. 1993.

[8] T. Randen and J. H. Husøy, "Novel approaches to multichannel filtering for image texture segmentation," in *SPIE Visual Comm. Image Proc. 1994*, vol. 2094, pp. 626–636, 1994.

[9] A. C. Bovik, "Analysis of multichannel narrowband filters for image texture segmentation," *IEEE Trans. Signal Processing*, vol. 39, no. 9, pp. 2025–43, Sept. 1991.

[10] D. F. Dunn and W. E. Higgins, "Optimal Gabor-filter design for texture segmentation," in *Proc. IEEE Int. Conf. Acoust., Speech, Signal Processing*, vol. V, pp. V37–V40, 1993.

[11] T. P. Weldon, W. E. Higgins, and D. F. Dunn, "Efficient Gabor filter design using Rician output statistics," *1994 IEEE Int. Symp. Circuits, Systems,* London, England, 30 May - 2 June, vol. 3, pp. 25–28, 1994.

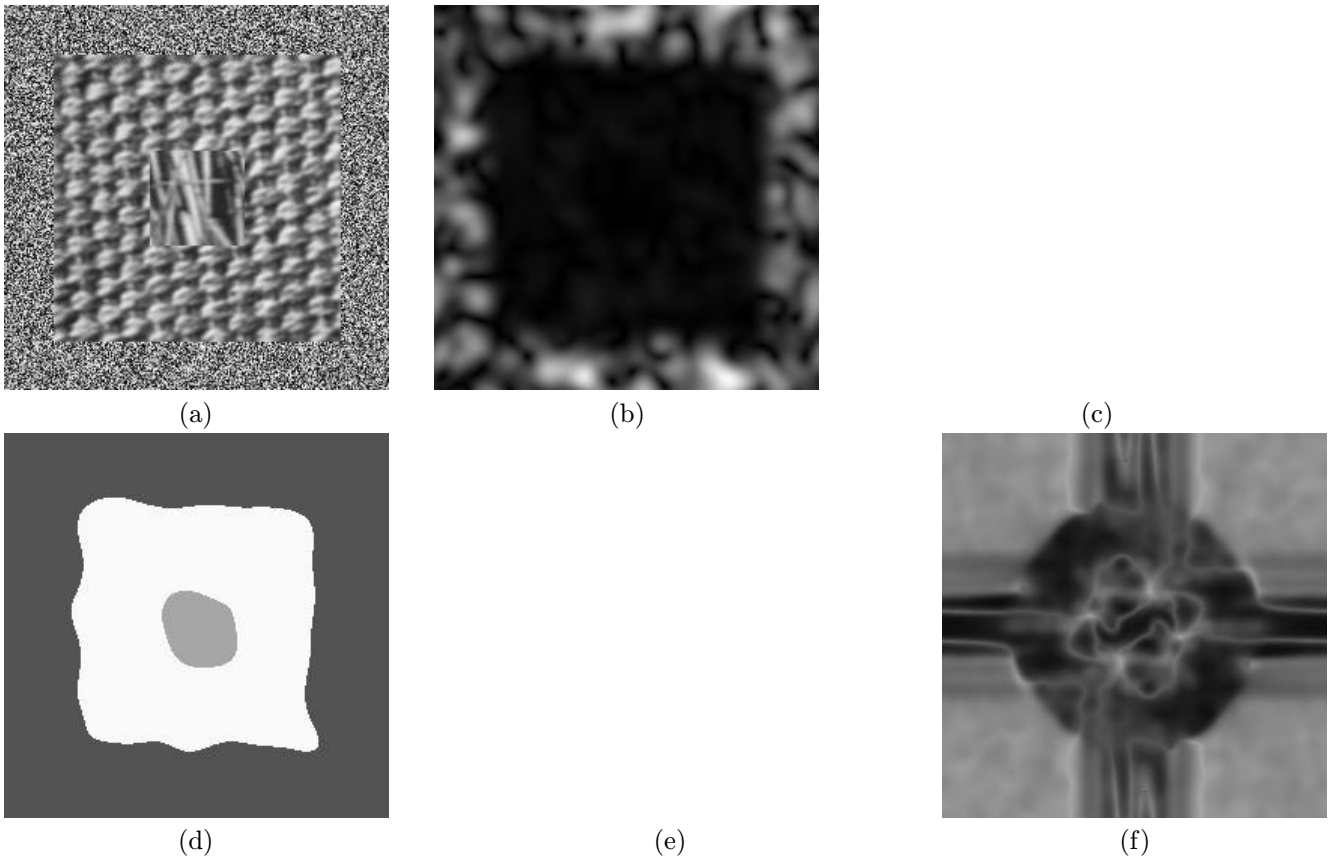

Figure 2: Results for optimal filter: (a) Input composite image: outer border is uniform noise, middle ring is straw (d77), interior square is cotton canvass (d15). (b) Prefilter magnitude $m(x, y)$, $(U, V) = (.18, .22)$ cycles/pixel, $\sigma_g = 5$. (c) Histogram of predicted (dashed) and actual (solid) $m(x, y)$. (d) Segmentation of postfiltered output, $\sigma_p = 8.5$, thresholds =.21,.63. (e) Histogram of predicted (dashed) and actual (solid) $m_p(x, y)$. (f) Segmentation error versus $(U, V)$, white=100%, black=0%; $(U, V) = (0, 0)$ at center of image.


[12] D. Dunn, W. Higgins, and J. Wakeley, "Texture segmentation using 2-D Gabor elementary functions," *IEEE Trans. Pattern Anal. and Machine Intell.*, vol. 16, no. 2, pp. 130–149, Feb. 1994.

[13] M. Schwartz, *Information Transmission, Modulation, and Noise*. New York, NY: McGraw-Hill, third ed., 1980.

[14] R. O. Duda and P. E. Hart, *Pattern Classification and Scene Analysis*. John Wiley and Sons, 1973.

[15] P. Brodatz, *Textures: A Photographic Album for Artists and Designers*. New York, NY: Dover, 1966.

[16] D. F. Dunn, T. P. Weldon, and W. E. Higgins, "Spectral anomalies in halftones and their impact on texture analysis," Tech. Rep. CSE-94-038, Penn State University, 1994.